

Synthesis and Characterization of an Inclusion Complex of DL-Aminoglutethimide with β -Cyclodextrin and Its Innovative Application in a Biological System: Computational and Experimental Investigations

Samapika Ray, Niloy Roy, Biraj Kumar Barman, Paramita Karmakar, Pranish Bomzan, Biplab Rajbanshi, Vikas Kumar Dakua, Ankita Dutta, Anoop Kumar, and Mahendra Nath Roy*



Cite This: *ACS Omega* 2022, 7, 11208–11216



Read Online

ACCESS |



Metrics & More

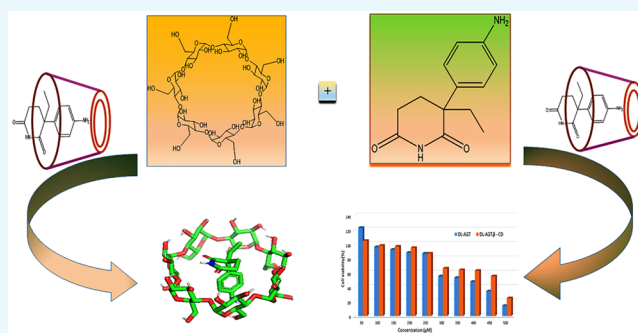


Article Recommendations



Supporting Information

ABSTRACT: Our present study intended to investigate the encapsulation of DL-AGT within the lipophilic cavity of a β -CD molecule. The consequential inclusion system was characterized by UV-visible spectroscopy and ^1H NMR, PXRD, SEM, and FT-IR studies. Molecular docking was performed for the inclusion complex to discover the most proper orientation, and it was seen that the drug DL-AGT fits into the cavity of β -CD in a 1:1 ratio, which was also confirmed from the Job plot. Furthermore, a comparison was done on the basis of cell viability between the drug and its inclusion complex.



1. INTRODUCTION

The drug DL-aminoglutethimide, (\pm)-3-(4-aminophenyl)-3-ethylpiperidine-2,6-dione (DL-AGT) (Scheme 1), used as an aromatase inhibitor for the treatment of advanced breast cancer and Cushing's syndrome was chosen as a suitable guest molecule for this study. According to the Biopharmaceutics Classification System, it is a class 11 drug with low water solubility but good permeability.¹ DL-Aminoglutethimide can cause aromatase inhibition. It was initially introduced as an anticonvulsant but due to its side effects of acting as a potent inhibitor of several enzymes on the adrenal cortex, it was no longer used. These drawbacks of this drug changed into a clinical advantage in the treatment of Cushing's syndrome and advanced breast cancer. The growth of certain tumors depends on specific hormones, and that makes the basis of endocrine therapy of breast cancer. DL-AGT is found to be effective in hormone-dependent breast carcinoma by suppressing the estrogen level in post-menopausal women. It inhibits the conversion of androgen to estrogen.² Moreover this drug is very effective in painful bone metastasis. However, aminoglutethimide has its side effects because of its toxicity,³ such as lethargy, depression, and rash, in addition to its benefits.⁴

Currently, molecular encapsulation is an important strategy to increase the bioavailability of certain drugs to retain their therapeutic activity. Potent drug delivery systems including biocompatible polymers and nanoparticles have already been explored. Cyclodextrin-based drug delivery systems are found to be the most prominent and reliable due to their nontoxicity

and biodegradability.^{5,6} Cyclodextrins or cycloamyloses are polymers with a truncated-cone-shaped cavity having a minimum number of six D(+)-glucopyranose units linked through α -1,4-bonds (Scheme 1).⁷ They can be natural or semisynthetic (oligosaccharides).⁸ The α -, β -, and γ -cyclodextrins and their derivatives have been extensively used in pharmaceutical science. For parental drug delivery, with oral administration, cyclodextrins have been extensively used. The applications of CDs are even more numerous than those above, as they are able to make inclusion complexes with some specific molecules which will fit in the cavity. Thus, the size of the entering guest molecule is also an important parameter here.⁹ The interactions between the host and the guest molecules are mainly noncovalent: e.g., ion-dipole, hydrogen-bonding and van der Waals types. The most widely accepted host for complex formation is β -CD due to its suitable cavity diameter and low production cost.^{10,11} β -Cyclodextrin consists of seven α -D-glucopyranose units joined by α -1,4-linkages.¹² Cyclodextrins are able to modify the pharmacological properties of the encapsulated active substances such as solubility,

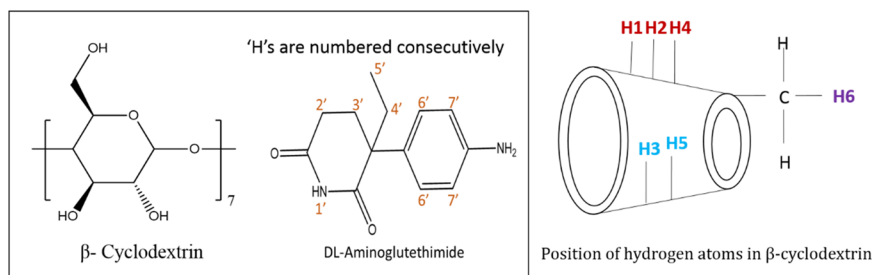
Received: January 5, 2022

Accepted: March 9, 2022

Published: March 28, 2022



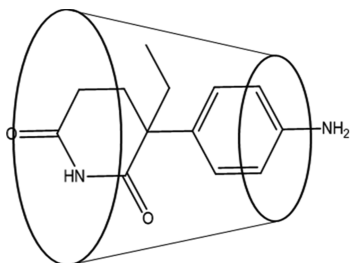
Scheme 1. Structures of the Studied Molecules



bioavailability, chemical stability, dispersibility, and toxicity; thus, by the preparation of inclusion complexes with cyclodextrin molecules it can be possible to enhance or improve such properties of the active compounds.^{13–16}

In our present work, encapsulation of DL-aminogluthethimide within the nanocavity of β -cyclodextrin was established by UV–vis, IR spectroscopic, powder X-ray diffraction, ¹H NMR, 2D ROESY, and scanning electron microscopic studies. A Job plot implies the stoichiometry of the complex to be 1:1, and a UV–visible study has given a proper explanation of the thermodynamic parameters of the inclusion process and association constant of the complex. Furthermore, an *in vitro* cell viability study between the drug and the inclusion complex showed that the inclusion complex is less toxic to a human normal kidney cell line in comparison to the drug. By the process of inclusion we are aiming toward the improvement of the properties of the drug (DL-AGT), i.e. to increase its solubility as it has low solubility, an enhancement of the specificity, and reduction of the toxicity. Most notably, the stability constant for the complexation of DL-AGT and β -CD by UV–visible spectroscopy has already been determined in the literature, though the whole project was on TM- β -CD and DL-AGT inclusion phenomena (Scheme 2).¹⁷

Scheme 2. Plausible Mechanism of Inclusion



2. RESULTS AND DISCUSSION

2.1. Job Plot. The stoichiometry of the host–guest inclusion complex can be determined with the help of a continuous variation method or a Job method.¹⁸ Here, a set of solutions of the drug (DL-AGT) and β -CD was prepared by varying the mole fraction of DL-AGT from 0 to 1, and by UV–vis spectroscopy the absorbances of all the solutions were checked at the λ_{\max} value (238 nm). By plotting $\Delta A \times R$ against R , a Job plot is generated, where ΔA is the difference in absorbances of the guest without and with β -CD and $R = [\text{DL-AGT}]/[\text{DL-AGT} + \beta\text{-CD}]$. The R_{\max} value obtained from the Job plot is 0.5 (Figure 1a), which signifies a 1:1 complexation of the guest and host molecule.¹⁹

2.2. Association Constants and Thermodynamic Parameters. The association constants of DL-AGT and β -CD IC were calculated at three different temperatures by UV–vis spectroscopy, measuring the change in the molar extinction coefficient of the guest molecule when it enters into the hydrophobic cavity of β -CD from the hydrophilic environment. The absorbance changes of DL-AGT were studied by gradually increasing the concentration of β -CD. The Benesi–Hildebrand equation is used for the determination of association constant¹⁸

$$\frac{1}{\Delta A} = \frac{1}{\Delta \epsilon [\text{AGT}]} \frac{1}{k_a [\text{CD}]} + \frac{1}{\Delta \epsilon [\text{AGT}]} \quad (1)$$

where $[\text{AGT}]$ and $[\text{CD}]$ are the concentrations of the guest molecule and the cyclodextrin molecule, $\Delta \epsilon$ refers to the change in the molar extinction coefficient, and ΔA is the change in the absorbance of DL-AGT on addition of CD. From the double-reciprocal plot of the Benesi–Hildebrand equation we have calculated the association constants at three different temperatures (293.15, 303.15, and 313.15 K), and the linearity of the plot suggests a 1:1 stoichiometry of the host and guest molecules.²⁰

Furthermore, the important thermodynamic parameters are determined from the plot of $\log k_a$ vs $1/T$ using eq 2.

$$2.303 \log k_a = -\frac{\Delta H^\circ}{RT} + \frac{\Delta S^\circ}{R} \quad (2)$$

The spontaneity of the reaction, i.e. the free energy change, is determined by eq 3

$$\Delta G^\circ = \Delta H^\circ - T\Delta S^\circ \quad (3)$$

where the symbols have their usual significance. Now the values of thermodynamic parameters suggest that the process of inclusion is exothermic, spontaneous, and entropy restricted (Table 1). This restriction in entropy may be due to the molecular association between the guest and host molecules.²¹

2.3. Solubility Study of DL-AGT- β -CD Inclusion Complex. The ethanolic solubility between pure DL-AGT and the DL-AGT- β -CD inclusion complex was evaluated using UV–visible spectroscopy.²² The UV–visible spectra of the DL-AGT- β -CD inclusion complex at different concentrations in ethanolic solutions are shown in Figure 2. As DL-AGT is sparingly soluble in water, the experiment was set up in the ethanolic phase and the solubility of DL-AGT in ethanol was greatly enhanced when the DL-AGT- β -CD inclusion complex was formed. DL-AGT displayed a maximum absorption peak (λ_{\max}) at about 238 nm in the inclusion complex, as shown in Figure 2A, and all of the calculations were carried out using the λ_{\max} value. It has been found that the peak positions during titration were independent of the concentrations of DL-AGT- β -CD but peak intensities increased upon an increase in

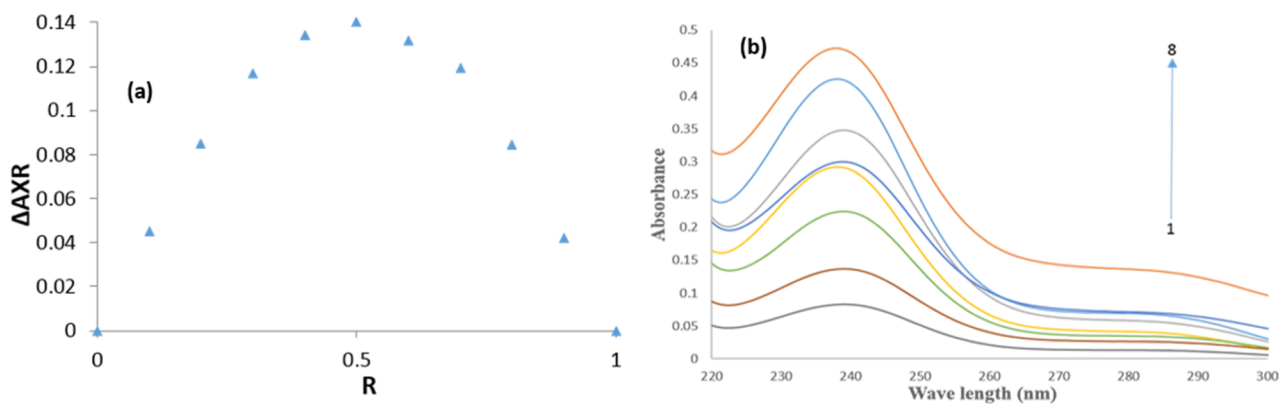


Figure 1. (a) Job plot for the stoichiometry 1:1 (host:guest) and (b) spectra of the Job plot.

Table 1. Association Constants (k_a), Gibbs Free Energy (ΔG°), Enthalpy (ΔH°) and Entropy (ΔS°) of an AGT- β -CD System from UV-Vis Spectroscopy

complex	k_a (10^3 M $^{-1}$)			ΔG° (kJ mol $^{-1}$)	ΔH° (kJ mol $^{-1}$)	ΔS° (J mol $^{-1}$) K $^{-1}$
	293.15 K	303.15 K	313.15 K			
DL-AGT- β -CD	3.55	2.54	1.59	-19.81	-30.59	-36.16

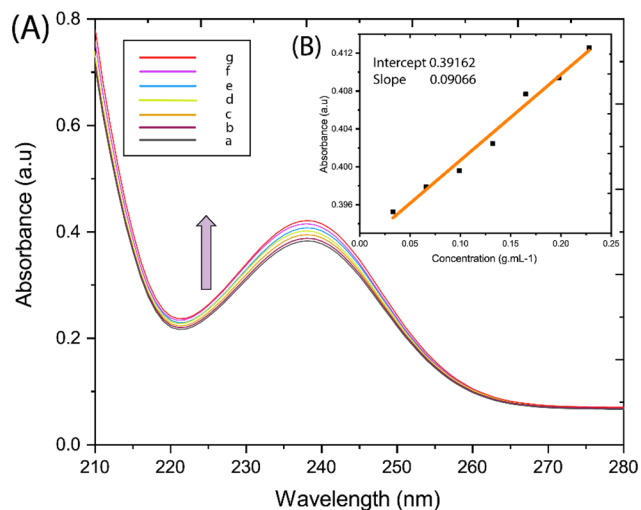


Figure 2. (A) UV spectra of DL-AGT- β -CD with different concentrations (g L $^{-1}$) in ethanolic solutions (at 298.15 K): (a) 0.033; (b) 0.066; (c) 0.099; (d) 0.132; (e) 0.165; (f) 0.198; (g) 0.228. (B) Plot of the absorbance of DL-AGT- β -CD at 238 nm vs the concentration of DL-AGT- β -CD.

concentration. The plot of the absorbance of DL-AGT- β -CD at 238 nm vs the concentration of DL-AGT- β -CD provides a straight line as shown in Figure 2B. According to the Lambert-Beer law, the molar extinction coefficient (ϵ) of DL-AGT- β -CD in ethanolic solution was evaluated to be 0.0907 L g $^{-1}$ cm $^{-1}$. The UV spectrum of the DL-AGT- β -CD inclusion complex at a saturated concentration in ethanolic solution is shown in the Figure S5, from which the absorbance value of a saturated solution of the DL-AGT- β -CD inclusion complex was calculated and found to be 1.59873. Finally, the solubilities of pure DL-AGT and DL-AGT- β -CD in ethanol at 25 °C are shown in the Table S5. Therefore, it was clear from the Table S5 that the DL-AGT- β -CD inclusion complex has greater a solubility of 17.62 mg mL $^{-1}$ in comparison to that of pure DL-AGT of 7 mg mL $^{-1}$. These results clearly imply that the water-soluble host β -CD played a critical role in

remarkably improving the solubility of the less soluble DL-AGT by the formation of the DL-AGT- β -CD inclusion complex. From the above we can also get a clear idea about the solubility of DL-AGT, as there was an enhancement in solubility in ethanol after inclusion.²³

2.4. PXRD Study. A diffractogram (Figure 3) of the DL-AGT- β -CD complex shows the disappearance of some of the pure DL-AGT spectral lines at 2θ values of 12.38, 15.09, 16.75, 17.95, and 24.92° and the β -CD spectral lines at 2θ values of 4.63, 9.11, and 12.63°, as shown in Table 2. Additionally, the appearance of new spectral lines of DL-AGT- β -CD complex at 2θ values of 17.85 and 18.50° is observed with less intense peaks. It is well-known that the peak at $2\theta = \sim 20^\circ$ in cyclodextrin-based inclusion complexes is a characteristic of “channel-type” packaging in β -CD where only the head-to-head arrangement has been observed. The disappearance of some peaks and the generation of new peaks with less intensity in the spectra of DL-AGT- β -CD inclusion complex suggest some types of interactions between the guest and host molecules.

2.5. FT-IR Spectroscopy. The formation of an inclusion complex can also be explained with the help of FT-IR spectroscopy. It is important to note that, when the inclusion complex is formed, several characteristic peaks of the guest molecule might shift, reduce, or disappear. The stretching and bending vibrations of the three components, viz. DL-AGT, β -CD, and their IC are shown in Figure 4.

In the case of DL-AGT, the most important bands present in the IR spectrum are those related to the imide and amino functional groups. The N-H, C-H, C-O, and C-N stretching modes give strong bands situated at 3500–3200, 2964, 1687, and 1202 cm $^{-1}$, respectively. The stretching at 3467 and 3375 cm $^{-1}$ may be due to the 1° and 2° amines, respectively, present in the drug molecule. The aromatic C=C stretching vibrations for DL-AGT were found at 1625, 1515, and 1448 cm $^{-1}$. Bending vibrations of -NH and -NH $_2$ appearing at 1625 cm $^{-1}$ display strong bands in the IR spectrum. However, in β -CD, the O-H stretching vibration appeared at 3424 cm $^{-1}$. The C-H stretching frequency for β -CD appeared at 2921 cm $^{-1}$, and the bending vibration of C-

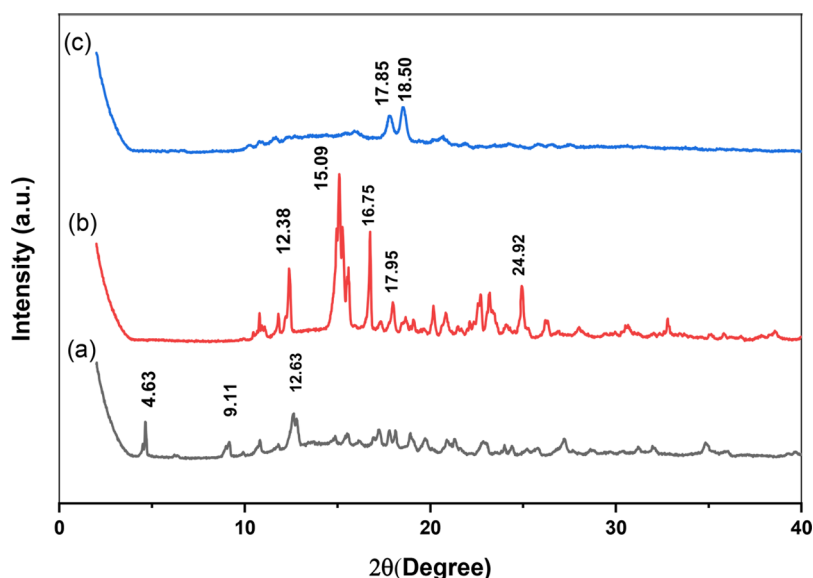


Figure 3. PXRD diffractograms of (a) β -CD, (b) DL-AGT, and (c) DL-AGT- β -CD IC (inclusion complex).

Table 2. 2θ Values of β -CD, DL-AGT, and DL-AGT- β -CD Inclusion Complex from PXRD Study

component	2θ (deg)
β -CD	4.63, 9.11, 12.63
DL-AGT	12.38, 15.09, 16.75, 17.95, 24.92
DL-AGT- β -CD IC	17.85, 18.50

O–C in β -CD appeared at 1153 cm^{-1} . When, the inclusion complex is formed, a broad hump is observed at 3388 cm^{-1} . The characteristic peak for C=O was observed at 1687 cm^{-1} in the case of DL-AGT, which was slightly shifted to 1693 cm^{-1} in the IC. In addition, the aromatic C=C stretching vibrations for DL-AGT in the complex were shifted to 1632 , 1515 , and 1454 cm^{-1} and the peak intensities were reduced to some extent. Thus, from the above explanation and from Figure 4, it is worth noting that most of the signals of β -CD and DL-AGT have been highly shifted with less peak intensity in the inclusion complex, implying some nonbonding interactions of the guest and host in the inclusion complex.

2.6. ^1H NMR Study. To predict the structure of the inclusion complex, ^1H NMR spectroscopy is a very useful method. It delivers detailed information about the positions of the H nuclei present in the structure of the molecule/complex of concern. As the host–guest inclusion process is based on weak nonbonding interactions, the changes occurring in the chemical shift values after inclusion are comparatively smaller than in other cases.²⁴

In β -CD, the H3 and H5 protons are located inside the cavity (H3 close to the wider rim and H5 close to the narrower rim) and H6 is outside the cavity, near the narrower rim.²⁵ When the guest molecule enters the cavity of β -CD, the protons inside the cavity (H3, H5) would definitely show some changes in chemical shift from that before.²⁶ It is observed that after inclusion the H3 and H5 protons of β -CD were shifted upfield but to a smaller extent. The ^1H NMR spectra of DL-AGT, β -CD, and the inclusion complex were shown in Figure 5. Numerous peaks were found in the spectrum of DL-AGT as well as in β -CD, which are given in Table 3. Chemical shift changes were calculated from the inclusion complex with

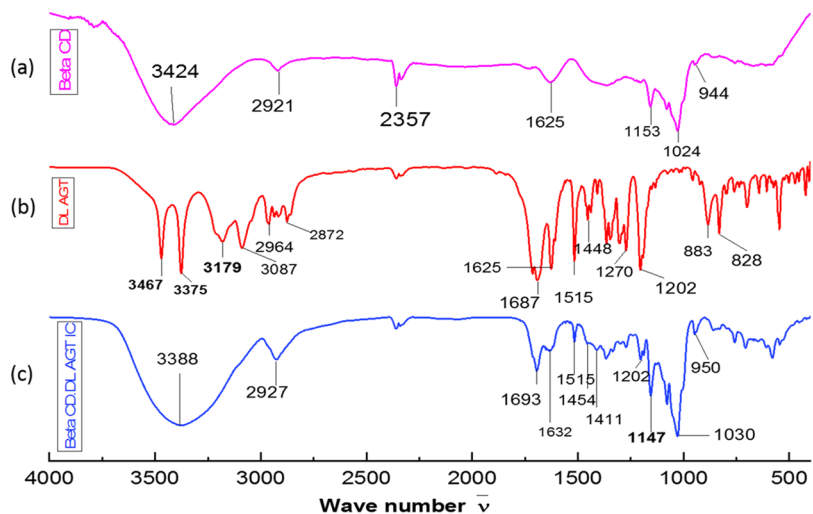


Figure 4. Infrared spectra of (a) β -CD, (b) DL-AGT, and (c) DL-AGT- β -CD IC (inclusion complex).

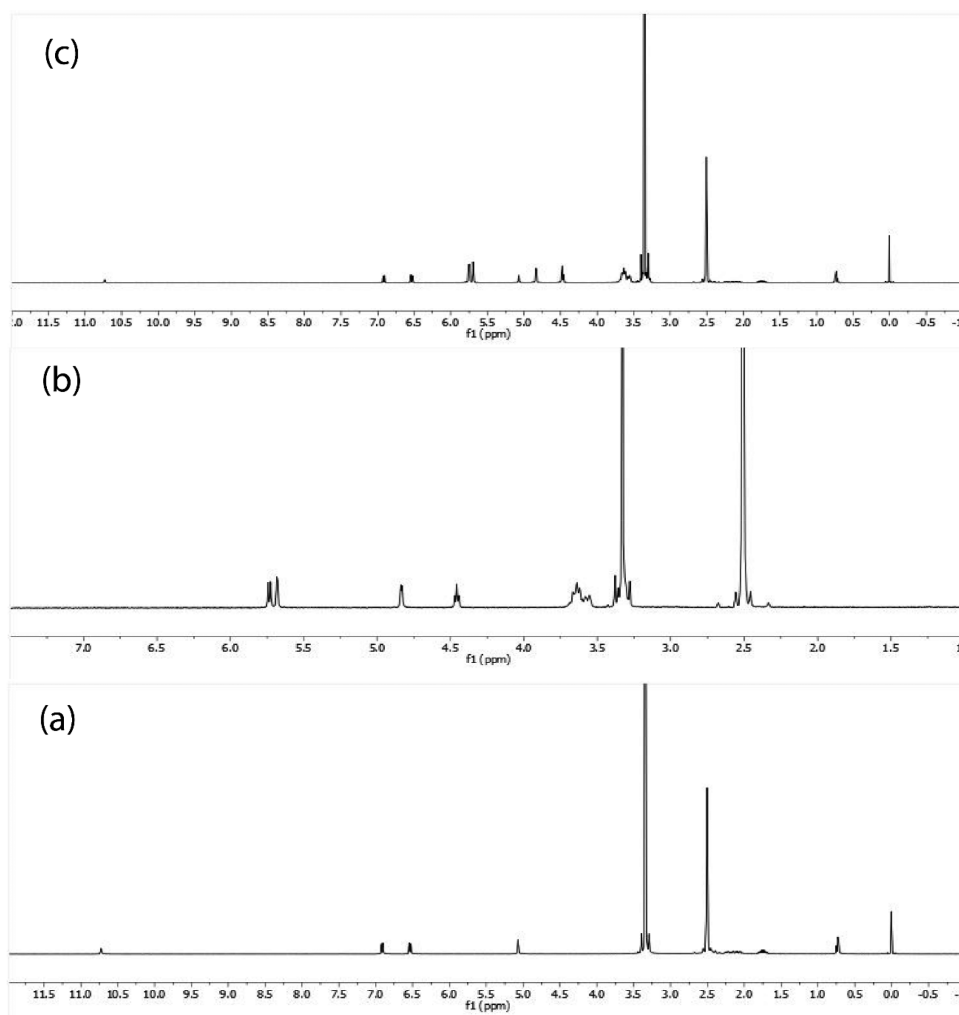


Figure 5. ^1H NMR spectra of (a) DL-AGT, (b) β -CD, and (c) DL-AGT $\cdot\beta$ -CD IC.

Table 3. Chemical Shifts and Their Deviations for the Protons of β -CD and of DL-AGT in Free State and in an Inclusion Complex

proton	chemical shift σ (ppm)			$\Delta\sigma$ ($\sigma_{\text{complex}} - \sigma_{\text{free}}$) ^a
	β -CD	DL-AGT	DL-AGT $\cdot\beta$ -CD	
H3	3.70		3.66	-0.04
H5	3.58		3.56	-0.02
H2'		5.11	5.07	-0.04
H3'		2.08	2.05	-0.03
H4'		1.81	1.78	-0.03
H5'		0.75	0.73	-0.02
H6'		6.93	6.93	0.0
H7'		6.55	6.55	0.0
Ar-NH ₂		10.73	10.73	0.0

^aNegative values of $\Delta\sigma$ indicate upfield shifts.

respect to both β -CD as well as DL-AGT as $\Delta\sigma = \sigma_{\text{complex}} - \sigma_{\text{DL-AGT}/\beta\text{-CD}}$. In case of β -CD, the upfield shift is greater for H3 (-0.04 ppm) than for H5 (-0.02 ppm). This result indicates that the inclusion occurred through the wider rim and that the H3 proton shifted more upfield than in comparison to the H5 proton. The signals related to the aromatic protons (H6', H7') of AGT remain almost constant in the spectrum of the inclusion complex. However, all the

protons related to the piperidine-2,6-dione moiety (H2', H3', H4', H5') are shifted upfield, as is shown in Table 3. Therefore, it can be concluded that only the nonaromatic parts were incorporated in the cavity of β -CD after complexation.

It is also evident from the MD studies that the aromatic part of DL-AGT is stabilized at the narrower end of the β -CD cavity. This is perhaps the reason for the absence of shifting of the aromatic protons of DL-AGT.

2.7. 2D-ROESY NMR Study. Two-dimensional (2D) NMR spectroscopy provides important information about the spatial arrangement between host and guest atoms by an observation of intermolecular dipolar cross correlations. If two protons are closely located in space, i.e., closer than 0.4 nm, this can produce a nuclear Overhauser effect (NOE) cross correlation in two-dimensional rotating-frame nuclear Overhauser enhancement correlation (2D-ROESY) spectroscopy, and therefore cross peaks in ROESY spectra will be obtained. The ROESY spectrum of the DL-AGT $\cdot\beta$ -CD complex (Figure 6) showed appreciable correlations of the H-3' and H-5' protons of DL-AGT with the H-3 and H-5 protons of β -CD. These results indicate that the piperidine-2,6-dione moiety of DL-AGT is in close proximity with the H-3 protons of β -CD. These results further confirmed that the DL-AGT $\cdot\beta$ -CD inclusion complex was successfully formed in the solution phase.

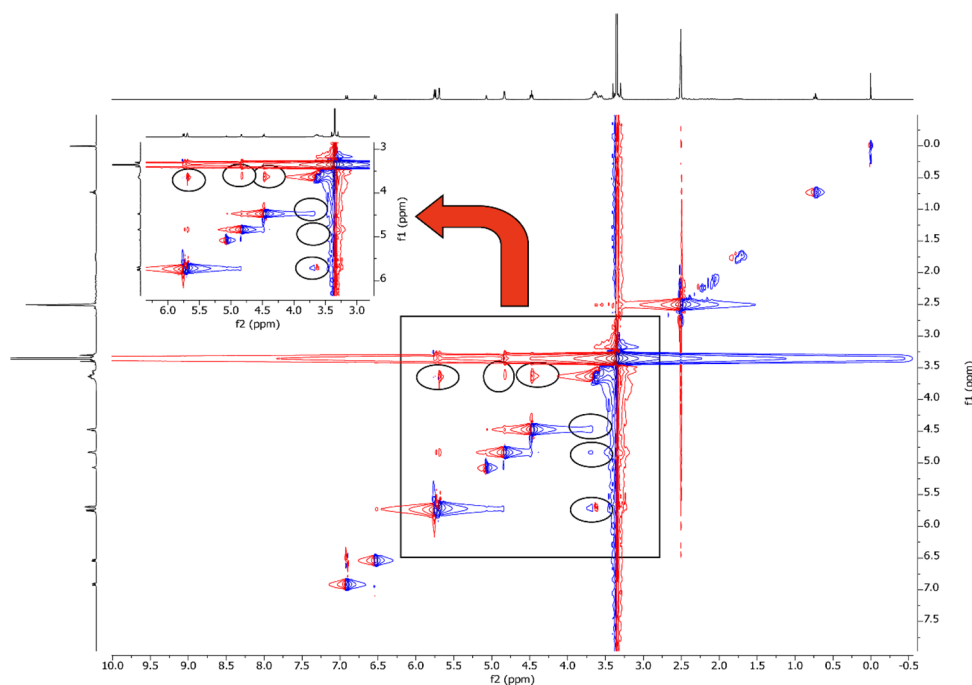


Figure 6. ROESY spectrum of β -CD.DL-AGT IC in d_6 -DMSO.

2.8. Molecular Docking Study. Molecular docking gives us effective information about bond simulations between molecules.²⁷ In order to comprehend the orientation, conformation, and interaction of the drug/guest molecule within the cavity of β -CD, molecular modeling is a constructive computational technique.²⁸

Here, docking has been used to predict the possible bound conformation of DL-AGT- β -CD inclusion complex and to estimate the binding affinity.²⁷ The drug within the binding cavity of β -CD was docked, and the most probable binding conformation was obtained.⁶ The results showed that the interaction between DL-AGT and β -CD is 1:1. The drug fit comfortably within the pocket, as shown in Figure 7. The

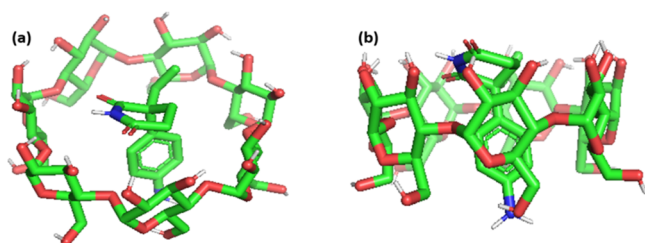


Figure 7. Mode of binding of the drug DL-AGT into β -CD (IC): (a) top view; (b) side view.

binding affinity for DL-AGT and β -CD was found to be -23.012 kJ/mol, as given in Table 4, which is in good agreement with the experimental findings from UV-vis spectroscopy. The results also indicated that in the complex only the piperidine-2,6-dione moiety of AGT interacted with

Table 4. Binding Affinity of DL-AGT and β -CD from Molecular Docking

ligand with receptor	binding affinity (ΔG° (kJ/mol))
DL-AGT- β -CD (IC)	-23.012

the H-3 protons of the CD cavity. The findings of this theoretical study are consistent with the results of FTIR and NMR experiments.

2.9. SEM Study. Scanning electron microscopy is one of the best techniques in describing the surface morphology of different chemical entities in the solid state. The surface morphologies of the host and guest and their inclusion complex are shown in Figure 8. Both DL-AGT and β -CD were found in crystal form in different sizes. However, DL-AGT appears as irregular-shaped crystal particles with large dimensions (Figure 8A), whereas β -CD has a polyhedral crystal like structure (Figure 8B). When complexation occurs, it is evident that the DL-AGT- β -CD IC (Figure 8C) exhibits a different surface morphology: a threadlike structure. This distinct surface morphology may be due to the formation of the inclusion complex.²¹ The totally dissimilar surface morphology of the inclusion complex may assist the other experimental observations.

2.10. In Vitro Cell Viability Study. The synthesized inclusion complex of the drug DL-AGT and β -CD and the drug itself were evaluated for a cell viability study. The cells were exposed to varying concentrations of the drug and inclusion complex, and the results of the cell viability obtained in the study are depicted graphically in Figure 9. After the drug treatment, the cell viability was found to be concentration dependent. In the case of the drug, as concentration increases, the cell viability of normal kidney cells decreases. However, the cells are more viable in the presence of the inclusion complex in comparison with the drug. This might be because of the higher toxicity of the drug (DL-AGT) at higher concentration (as the amount of the drug increases), where normal cells lose their reproducibility and eventually die. However, for the inclusion complex the cell viability is greater than that of the original drug as we move from lower to higher concentration. Thus, it is worth mentioning that the complex is less toxic in nature than the drug itself and so the cells are able to grow and reproduce properly. This finding clearly indicates the fact that

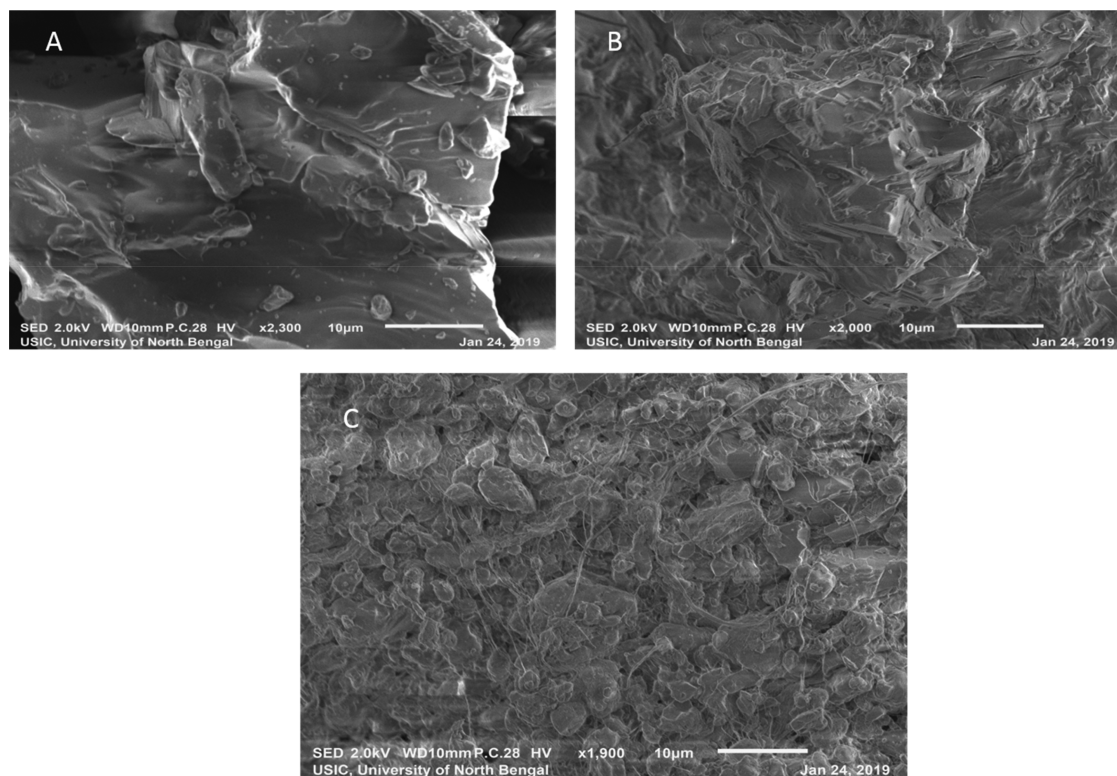


Figure 8. SEM images of (A) DL-AGT (B) β -CD and (C) DL-AGT- β -CD IC.

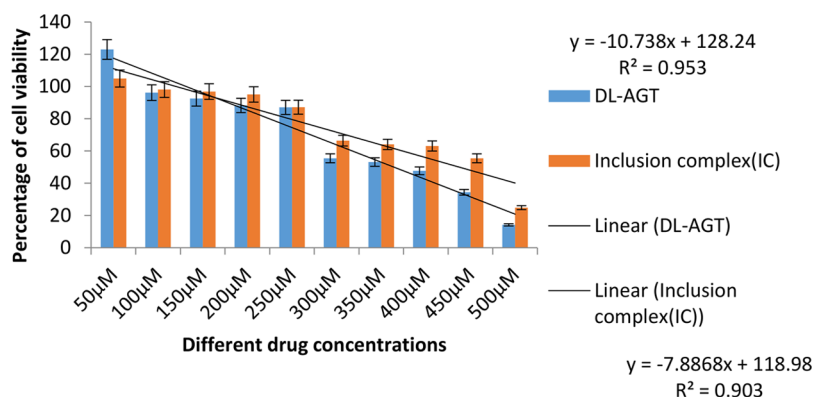


Figure 9. *In vitro* cell viability study of pure drug and its inclusion complex.

the inclusion complex is less toxic, as it causes less antiproliferative activity of cell in comparison to the drug. This behavior of the inclusion complex might be due to the controlled release of the drug from the cavity of β -CD.¹⁴

3. CONCLUSION

In our present study we have synthesized an attainable inclusion complex of the aromatase inhibitory drug DL-AGT and the host β -CD. The process of inclusion was confirmed by ¹H NMR, PXRD, FTIR, SEM, and UV-vis studies. From the Job plot (UV-visible study) and from the shifting of the H3 and H5 protons of β -CD in the ¹H NMR spectra of the IC, it is confirmed that the inclusion occurred in a 1:1 stoichiometric ratio. Moreover, the solubility of the IC in ethanol being greater than that of the pure drug was also determined. The above experimental observations were further affirmed by a molecular docking study, which helps to predict the most stable conformation of the inclusion complex. Finally, a cell

viability study between the drug and its IC with β -CD implies that, when the concentration is increased, the inclusion complex shows less toxicity than the drug itself. Thus, this is an important finding about the inclusion complex of the drug with β -CD, which may improve the therapeutic activity of the drug toward the application it is meant for and also could change the path of science to a new direction.

4. EXPERIMENTAL SECTION

4.1. Materials. The drug DL-AGT (purity >98%, molecular weight 232.28 g/mol) was purchased from TCI chemicals India PVT. Ltd. β -CD (purity \geq 97%; molecular weight 1134.98 g/mol) was purchased from Sigma-Aldrich Germany. All reagents were used without further purification.

4.2. Methods. DL-Aminoglutemide and β -CD were weighed using a Mettler Toledo AG-285 apparatus (uncertainty \pm 0.1 mg), and they were prepared in a 15% acetonitrile solution (acetonitrile-water mixture) at 298.15

K. Other solutions of the required strengths were prepared by mass dilution.

Fourier transform infrared (FTIR) spectra of DL-AGT, β -CD, and the DL-AGT- β -CD inclusion complex were recorded on a PerkinElmer 8300 FT-IR spectrometer (PerkinElmer, Inc., Germany) using the KBr disk technique. Samples were prepared as thin KBr disks using a 1:100 ratio of sample to KBr. The range of scanning was kept at 4000–400 cm^{-1} . ^1H NMR spectra were obtained using a Bruker AVANCE NEO 400 MHz (Bruker Inc., Germany) instrument in DMSO- d_6 solvent medium, where the solvent residual peak was taken as an internal standard. UV–visible titration for the Job plot as well as the determination of the association constant were carried out with an Agilent 8453 spectrophotometer (USA). PXRD data were obtained with Bruker D8 Advance instrument (Germany) having a Cu $K\alpha$ radiation source with 45 kV and $\lambda = 1.5406 \text{ \AA}$, and the scanning range was from 5° to 80° . The scanning electron micrographs were determined with JEOL JSM-IT 100 scanning electron microscope.

4.3. Molecular Docking. A molecular docking process was employed through PyRx software for the virtual screening of the small guest molecule (DL-AGT) and the host (β -CD) to find the geometry of the inclusion complex.²⁹ This software is written in the Python programming language with an in-built user interface that can be easily operated on all major operating systems (Linux, Windows, and Mac OS) and used to determine the binding parameters as well as binding geometry. PyRx uses Vina and AutoDock 4.2 as docking software. The input files for the host and guest were initially in the .pdb format and changed to .pdbqt files using in-built AutoDock Vina software. Once all the files were prepared, they were subjected to docking by means of AutoDock Vina. Before the docking calculation was started, a grid box was prepared around the host molecule. This resulted in a binding site centers of 8.3636, 24.4146, and 1.2278 for the x , y , and z axes, respectively. Grid box dimensions for the x , y , and z conformations were fixed at 25, 25, and 25, respectively. The grid space size was allocated perfectly, which allows selecting a search space for the host to perform docking with the guest, normally, at the most probable binding site. The interaction between DL-AGT and β -CD was determined on the basis of the Lamarckian genetic algorithm (LGA). Once the calculations were ended, the binding affinity (kJ mol^{-1}) of the most stable conformation of the host with the guest was provided by the software and is given in Table 4.³⁰

4.4. In Vitro Cell Viability Study. The cell viability study of the drug and the synthesized complex was investigated by an MTT assay. HEK-293 (human normal kidney cell line) was cultured in a 96-well microtiter plate at 37°C , in the presence of 5% carbon dioxide (CO_2), at a density of 5×10^3 cells/well in 100 μL of DMEM (Dulbecco's Modified Eagle Medium) Ham F-12 culture medium. After 24 h of incubation, the drugs (DL-AGT, DL-AGT- β -CD) were added in each well at different concentrations (50, 100, 150, 200, 250, 300, 350, 400, 450, and 500 μM) in triplicate. Then, the microtiter plate was incubated under the same experimental conditions. The next day, after the culture media were discarded from the treated plate 10 μL (5 mg/mL) of MTT powder (3-(4,5-dimethylthiazol-2-yl)-2,5-diphenyltetrazolium bromide) dissolved in 1X PBS was added to each well. The plate was again kept in the incubator for 3 h under the aforementioned conditions. Finally, a formazan solubilizer, i.e. isopropanol, was added to each well containing MTT solution and the plate was

shaken for about 10 min. Finally, the absorbance was recorded by a microtiter plate reader (SPECTROstar^{Nano}, Germany) at 620 nm.³¹ Solutions of the samples were prepared in DMSO.³²

4.5. Preparation of Inclusion Complex. By mixing β -CD and DL-ADT in a molar ratio of 1:1, the IC was prepared. A 1.0 mmol portion of DL-AGT was dissolved in 25 mL of 15% acetonitrile and 1.0 mmol of β -CD in 25 mL of distilled water. While the β -CD solution was kept on a magnetic stirrer, the DL-AGT guest solution was added slowly and the mixture was stirred for 36 h at constant temperature of 50°C . The suspension thus obtained was filtered and dried in an oven at 70°C for 7 h. Ultimately the solid powder was collected and stored in a desiccator for future use.

■ ASSOCIATED CONTENT

Supporting Information

The Supporting Information is available free of charge at <https://pubs.acs.org/doi/10.1021/acsomega.2c00011>.

Data of Job plot, Benesi–Hildebrand double-reciprocal plot, and plot of $\log k_a$ vs $1/T$ (PDF)

■ AUTHOR INFORMATION

Corresponding Author

Mahendra Nath Roy – University of North Bengal, Department of Chemistry, Darjeeling, West Bengal, India 734013; Alipurduar University, Department of Chemistry, Alipurduar, West Bengal, India 736122; orcid.org/0000-0002-7380-5526; Email: mahendraroy2002@yahoo.co.in

Authors

Samapika Ray – University of North Bengal, Department of Chemistry, Darjeeling, West Bengal, India 734013

Niloy Roy – University of North Bengal, Department of Chemistry, Darjeeling, West Bengal, India 734013

Biraj Kumar Barman – Parimal Mitra Smriti Mahavidyalaya, Department of Chemistry, Jalpaiguri, West Bengal, India 735221

Paramita Karmakar – University of North Bengal, Department of Chemistry, Darjeeling, West Bengal, India 734013

Pranish Bomzan – University of North Bengal, Department of Chemistry, Darjeeling, West Bengal, India 734013

Biplab Rajbanshi – University of North Bengal, Department of Chemistry, Darjeeling, West Bengal, India 734013

Vikas Kumar Dakua – Alipurduar University, Department of Chemistry, Alipurduar, West Bengal, India 736122

Ankita Dutta – University of North Bengal, Department of Biotechnology, Darjeeling, West Bengal, India 734013

Anoop Kumar – University of North Bengal, Department of Biotechnology, Darjeeling, West Bengal, India 734013

Complete contact information is available at:

<https://pubs.acs.org/doi/10.1021/acsomega.2c00011>

Funding

This research received no specific grant from any funding agency in the public, commercial, or not-for-profit sectors.

Notes

The authors declare no competing financial interest.

■ ACKNOWLEDGMENTS

Authors express their gratitude to UGC-SAP, Department of Chemistry, University of North Bengal. Authors are highly

indebted to the Department of Biotechnology, University of North Bengal for the Cell viability study.

ABBREVIATIONS:

DL-AGT:DL-aminoglutethimide

β -CD: β -cyclodextrin

IC:inclusion complex

FTIR:fourier Transform infrared spectroscopy

NMR:nuclear magnetic resonance

PXRD:powder X-ray crystal diffraction

REFERENCES

- (1) Mitran, R. A.; Nastase, S.; Matei, C.; Berger, D. Tailoring the dissolution rate enhancement of aminoglutethimide by functionalization of MCM-41 silica: a hydrogen bonding propensity approach. *RSC Adv.* **2015**, *5* (4), 2592–2601.
- (2) Miller, W. Aromatase inhibitors. *Endocr.-Relat. Cancer.* **1996**, *3* (1), 65–79.
- (3) Lønning, P. The potency and clinical efficacy of aromatase inhibitors across the breast cancer continuum. *Ann. Oncol.* **2011**, *22* (3), 503–514.
- (4) Smith, I. E.; Harris, A. L.; Morgan, M.; Gazet, J. C.; McKinna, J. A. Tamoxifen versus aminoglutethimide versus combined tamoxifen and aminoglutethimide in the treatment of advanced breast carcinoma. *Cancer Res.* **1982**, *42* (8), 3430s–3432s.
- (5) Yang, Y.; Gao, J.; Ma, X.; Huang, G. Inclusion complex of tamibarotene with hydroxypropyl- β -cyclodextrin: Preparation, characterization, in-vitro and in-vivo evaluation. *Asian J. Pharm. Sci.* **2017**, *12* (2), 187–192.
- (6) Tom, L.; Nirmal, C. R.; Dusthacker, A.; Magizhaveni, B.; Kurup, M. Formulation and evaluation of β -cyclodextrin-mediated inclusion complexes of isoniazid scaffolds: molecular docking and in vitro assessment of antitubercular properties. *New J. Chem.* **2020**, *44* (11), 4467–4477.
- (7) Gandhi, S. R.; Quintans, J. D. S. S.; Gandhi, G. R.; Araújo, A. A. D. S.; Quintans Junior, L. J. The use of cyclodextrin inclusion complexes to improve anticancer drug profiles: a systematic review. *Expert Opin Drug Delivery* **2020**, *17* (8), 1069–1080.
- (8) Giordano, F.; Novak, C.; Moyano, J. R. Thermal analysis of cyclodextrins and their inclusion compounds. *Thermochim. Acta* **2001**, *380* (2), 123–151.
- (9) Haihem, S.; Nouar, L.; Djilani, I.; Bouhadiba, A.; Madi, F.; Khatmi, D. E. Host-guest inclusion complex between β -cyclodextrin and paeonol: A theoretical approach. *C R Chim.* **2013**, *16* (4), 372–379.
- (10) Singh, U.; Aithal, K.; Udupa, N. Physicochemical and Biological Studies of Inclusion Complex of Methotrexate with β -Cyclodextrin. *Pharmacol. Commun.* **1997**, *3* (12), 573–577.
- (11) Liu, Y.; Chen, G. S.; Chen, Y.; Lin, J. Inclusion complexes of azadirachtin with native and methylated cyclodextrins: solubilization and binding ability. *Bioorg. Med. Chem.* **2005**, *13* (12), 4037–4042.
- (12) D'Aria, F.; Serri, C.; Niccoli, M.; Mayol, L.; Quagliariello, V.; Iaffaioli, R. V.; Biondi, M.; Giancola, C. Host-guest inclusion complex of quercetin and hydroxypropyl- β -cyclodextrin. *J. Therm. Anal. Calorim.* **2017**, *130* (1), 451–456.
- (13) Butnariu, M.; Peana, M.; Sarac, I.; Chirumbolo, S.; Tzoupis, H.; Chasapis, C. T.; Bjørklund, G. Analytical and in silico study of the inclusion complexes between tropane alkaloids atropine and scopolamine with cyclodextrins. *Chem. Pap.* **2021**, *75*, 5523–5533.
- (14) Bomzan, P.; Roy, N.; Sharma, A.; Rai, V.; Ghosh, S.; Kumar, A.; Roy, M. N. Molecular encapsulation study of indole-3-methanol in cyclodextrins: Effect on antimicrobial activity and cytotoxicity. *J. Mol. Struct.* **2021**, *1225*, 129093.
- (15) Paczkowska, M.; Mizera, M.; Szymanowska-Powalowska, D.; Lewandowska, K.; Błaszczak, W.; Gościńska, J.; Pietrzak, R.; Cielecka-Piontek, J. β -Cyclodextrin complexation as an effective drug delivery system for Meropenem. *Eur. J. Pharm. Biopharm.* **2016**, *99*, 24–34.
- (16) Al Azzam, K. M.; Muhammad, E. Host-guest inclusion complexes between mitoglinide and the naturally occurring cyclodextrins α , β , and γ : a theoretical approach. *Adv. Pharm. Bull.* **2015**, *5* (2), 289.
- (17) Nowakowski, M.; Dlugosz, M.; Taraszewska, J.; Wojcik, J. Complexation of aminoglutethimide with native and modified cyclodextrins. *J. Phys. Org. Chem.* **2009**, *22* (10), 948–953.
- (18) Saha, S.; Roy, A.; Roy, M. N. Mechanistic Investigation of Inclusion Complexes of a Sulfa Drug with α - and β -Cyclodextrins. *Ind. Eng. Chem. Res.* **2017**, *56* (41), 11672–11683.
- (19) Saha, S.; Roy, A.; Roy, K.; Roy, M. N. Study to explore the mechanism to form inclusion complexes of β -cyclodextrin with vitamin molecules. *Sci. Rep.* **2016**, *6* (1), 1–12.
- (20) Barman, S.; Barman, B. K.; Roy, M. N. Preparation, characterization and binding behaviors of host-guest inclusion complexes of metoclopramide hydrochloride with α - and β -cyclodextrin molecules. *J. Mol. Struct.* **2018**, *1155*, 503–512.
- (21) Rajbanshi, B.; Dutta, A.; Mahato, B.; Roy, D.; Maiti, D. K.; Bhattacharyya, S.; Roy, M. N. Study to explore host guest inclusion complexes of vitamin B1 with CD molecules for enhancing stability and innovative application in biological system. *J. Mol. Liq.* **2020**, *298*, 111952.
- (22) Ghosh, B.; Roy, N.; Roy, D.; Mandal, S.; Ali, S.; Bomzan, P.; Roy, K.; Roy, M. N. An extensive investigation on supramolecular assembly of a drug (MEP) with β CD for innovative applications. *J. Mol. Liq.* **2021**, *344*, 117977.
- (23) Zhang, W.; Gong, X.; Cai, Y.; Zhang, C.; Yu, X.; Fan, J.; Diaoy, G. Investigation of water-soluble inclusion complex of hypericin with β -cyclodextrin polymer. *Carbohydr. Polym.* **2013**, *95* (1), 366–370.
- (24) Usacheva, T. R.; Volynkin, V. A.; Panyushkin, V. T.; Lindt, D. A.; Pham, T. L.; Nguyen, T. T. H.; Le, T. M. H.; Alister, D. A.; Kabirov, D. N.; Kuranova, N. N.; et al. Complexation of Cyclodextrins with Benzoic Acid in Water-Organic Solvents: A Solvation-Thermodynamic Approach. *Molecules* **2021**, *26* (15), 4408.
- (25) Thi, T. D.; Nauwelaerts, K.; Froeyen, M.; Baudempez, L.; Van Speybroeck, M.; Augustijns, P.; Annaert, P.; Martens, J.; Van Humbeeck, J.; Van Den Mooter, G. Comparison of the complexation between methylprednisolone and different cyclodextrins in solution by 1H-NMR and molecular modeling studies. *J. Pharm. Sci.* **2010**, *99* (9), 3863–3873.
- (26) Zhao, X.; Xiao, D.; Alonso, J. P.; Wang, D. Y. Inclusion complex between beta-cyclodextrin and phenylphosphonicdiamide as novel bio-based flame retardant to epoxy: Inclusion behavior, characterization and flammability. *Mater. Des.* **2017**, *114*, 623–632.
- (27) Rezende, A. A.; Santos, R. S.; Andrade, L. N.; Amaral, R. G.; Pereira, M. M.; Bani, C.; Chen, M.; Priefer, R.; da Silva, C. F.; de Albuquerque Júnior, R. L.; et al. Anti-tumor efficiency of perillyl alcohol/ β -cyclodextrin inclusion complexes in a sarcoma S180-induced mice model. *Pharmaceutics* **2021**, *13* (2), 245.
- (28) Mady, F. M.; Aly, U. F. Experimental, molecular docking investigations and bioavailability study on the inclusion complexes of finasteride and cyclodextrins. *Drug Des. Devel. Ther.* **2017**, *11*, 1681.
- (29) Dallakyan, S.; Olson, A. J. *Small-molecule library screening by docking with PyRx, Chemical biology*; Springer: 2015; pp 243–250.
- (30) Parray, Z. A.; Ahmad, F.; Hassan, M. I.; Hasan, I.; Islam, A. Effects of Ethylene Glycol on the Structure and Stability of Myoglobin Using Spectroscopic, Interaction, and In Silico Approaches: Monomer Is Different from Those of Its Polymers. *ACS Omega* **2020**, *5* (23), 13840–13850.
- (31) Denizot, F.; Lang, R. Rapid colorimetric assay for cell growth and survival: modifications to the tetrazolium dye procedure giving improved sensitivity and reliability. *J. Immunol. Methods* **1986**, *89* (2), 271–277.
- (32) Mondal, M.; Basak, S.; Roy, D.; Saha, S.; Ghosh, B.; Ali, S.; Ghosh, N. N.; Dutta, A.; Kumar, A.; Roy, M. M. Cyclic oligosaccharides as controlled release complexes with food additives (TZ) for reducing hazardous effects. *J. Mol. Liq.* **2022**, *348*, 118429.